

Maejo Int. J. Sci. Technol. **2010**, 4(03), 405-416

Maejo International Journal of Science and Technology

ISSN 1905-7873

Available online at www.mijst.mju.ac.th

Full Paper

Segmentation and feature extraction of fluid-filled uterine fibroid—A knowledge-based approach

Ratha Jeyalakshmi^{1,*} and Ramar Kadarkarai²

¹ Mother Teresa Women's University, Kodaikanal, Tamil Nadu, India

² Computer Science and Engineering Department, National Engineering College, Kovilpatti, Tamil Nadu, India

* Corresponding author, e-mail: radha_jeyalakshmi@yahoo.com

Received: 22 February 2010 / Accepted: 28 September 2010 / Published: 5 October 2010

Abstract: Uterine fibroids are the most common pelvic tumours in females. Ultrasound images of fibroids require image segmentation and feature extraction for analysis. This paper proposes a new method for segmenting the fluid-filled fibroid found in the uterus. It presents a fully automatic approach in which there is no need for human intervention. The method used in this paper employs a number of knowledge-based rules to locate the object and also utilises the concepts in mathematical morphology. It also extracts the necessary features of the fibroid which can be used to prepare the radiological report. The performance of this method is evaluated using area-based metrics.

Keywords: uterine fibroid, ultrasound images, mathematical morphology

INTRODUCTION

Ultrasound imaging is widely used in the field of medicine. It is used for imaging soft tissues in organs such as liver, kidney, spleen, uterus, heart and brain. Ultrasound imaging is a common modality used for detecting fibroids. The most noticeable advantages of ultrasound scanning are safety, cost effectiveness, speed, easy handling and portability. Ultrasound is based on the principle of sound wave echoes. Sound wave travels from the probe to the object, passes through it and is continuously reflected back to the probe from multiple points inside the object. Ultrasound involves sound wave of frequency in the range of megahertz; typically this ranges between 3.5-10 MHz. The reflected sound wave is converted back to electrical signals in the probe and transmitted to the processing device which displays the image on the monitor. Bright or white areas in the image represent high reflectivity

or reflective surfaces/interphases in the body. Bone, air and calcium containing lesions (e.g. stone) appear intensely bright (whiter) or hyperechoic. Blacker or low signal reflection areas are called hypoechoic. Anechoic structures are usually filled structures like blood, urine, etc. Such structures as the liver, pancreas and uterus appear in various shades of gray depending upon their echogenicity (ability to reflect ultrasound waves). If a tissue allows sound wave to be transmitted so well that no echo can be detected, it is called anechoic and it appears as a dark and uniform region on an ultrasound image because there is no echo to give the intensity and texture. Because water has a much lower acoustic impedance ($1.48 \times 10^6 \text{ kg/m}^2/\text{s}$) than an average soft tissue ($1.63 \times 10^6 \text{ kg/m}^2/\text{s}$) [1], fluid-filled collections such as cysts are often anechoic and appear as dark regions with well-defined boundaries. The echogenicity of the tissues on which the ultrasound waves fall differs with respect to the texture of the tissues.

In this paper automatic segmentation of uterine fibroids is performed. Fibroids are muscular tumours that grow in the uterus. Another medical term for fibroids is "leiomyoma" or just "myoma". Fibroids are almost always benign (not cancerous). Anyhow, the symptoms caused by a fibroid may cause certain inconvenience in women and need to be treated. The fibroid may be in different textures. There is a type of fibroid most of whose portion is filled with fluid and the remaining portion consists of soft tissues. The fluid part appears dark and all the pixels have a minimum intensity. Some fibroids may have soft tissues for the entire portion. There is another type of fibroid which sticks to the wall of the uterus which is near the urinary bladder. This can be identified by the hyperechoic part which projects into the urinary bladder. The remaining portion contains both fluid and soft tissues. In a fluid-filled fibroid, the major portion of the tumour is fluid and therefore it is anechoic. Still another type of fibroid is fully or partially calcified and found anywhere inside the uterus. The calcified part appears hyperechoic. The proposed algorithm in this paper deals with segmentation of the fluid-filled fibroids.

The quality of ultrasound images is limited by granular speckle noise. This makes it difficult to segment the images. In this paper, the image is preprocessed in order to crop it such that unnecessary portions as well as the speckle noise are removed. We use a morphological cleaning algorithm to clean the image. Then it is segmented by an algorithm which uses a collection of rules to locate the fibroid and morphological concepts to segment the image. Finally, essential features are extracted, which might be useful for treating an abnormality.

Various techniques for speckle noise removal are available in the literature [2-6]. There are many segmentation algorithms for segmenting medical images [7]. There is a survey of ultrasound image segmentation [8]. Various introduced methods for segmenting ultrasound images are fully automatic [9-12].

A hybrid segmentation method based on morphological operators and a Gaussian function constraint to delimitate the tumour search scope, both used for tumour segmentation purposes, was proposed [8]. A new automatic seed point selecting method for new region growing algorithm was proposed for breast lesions [9]. A region-based segmentation method for ultrasound images using local statistics [10] produces results that are less sensitive to the pixel location and it also allows a segmentation of the accurate homogeneous regions. An automatic process of filtering, segmenting and analysing the features of breast nodules in ultrasound images was presented [11]. Anisotropic diffusion filter to suppress speckle noise and radial derivative function to segment the breast lesion in breast

ultrasound images were presented [12]. There are a number of research work which use watershed segmentation [13-16]. To solve the over-segmentation problem associated with this method, different techniques have been used [13-14, 16, 19]. There are also research papers on the application of morphological concepts to image segmentation [17-19]. There are papers which deal with rule-based segmentation algorithm [20-22]. Only two research papers are found, which focus on uterine fibroid segmentation [23-24], but they involve work on MRI images. There is apparently no work on ultrasound images of uterine fibroid.

METHODS

Preprocessing

The preprocessing of an original ultrasound image consists of two steps, namely cropping the image and removing the speckle noise.

Cropping image

The image contains the details of the patient on the top. The left-hand side and right-hand side contain other details, viz. scale, type of scan, frequency used, diameter of tumour, etc. The view of the image is not always the same. The radiologist uses the one which shows the object of interest clearly. In some images, we found the urinary bladder occupying one quarter of the image in the upper part where the uterus was below the urinary bladder and the fibroid was on the lower part of the uterus. In such cases, the part from the upper portion of the image to the bladder should be cropped as shown in Figure 1. The uterus area should be defined from below the ending row of the urinary bladder to the end of the image.



Figure 1. (a) Original image before cropping; (b) Image after cropping

In some images, the uterus was located in the upper portion of the image and a small portion of the bladder was visible on the right-hand side of the upper portion of the image. In such cases, the fibroid could be observed in the upper half of the image. Hence, a hundred rows from the bottom of the image should be removed from the image as shown in Figure 2. These areas of the image could be cropped. The top of the image below the detailed area showed the skin and flat layer of the abdomen. So these areas could also be cropped.

Speckle noise cleaning

A modified morphological image cleaning (MMIC) algorithm was used for cleaning the image. This is the modified version of morphological image cleaning (MIC) algorithm [3]. This algorithm

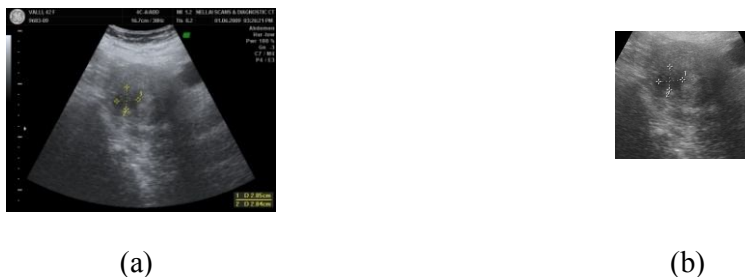


Figure 2. (a) Original image where uterus is located in the upper portion; (b) Image after cropping

works as follows. Initially, we define three arbitrary structuring elements with different sizes which resemble the shape of the speckles found in the image. Using these structuring elements (shown in Figure 3), a series of operations such as opening-closing followed by closing-opening is done to remove speckle noise. The top hat and bottom hat of this filtered image is found and they are binarised separately. These two binary images are reconstructed in order to get back the features that are lost while filtering. To reconstruct the features that are lost while cleaning, grayscale opening by reconstruction and grayscale closing by reconstruction are used. These are efficient techniques for getting back the lost image features [2].

001100	000000000000	00000000000000
011111	000111100000	00001111000000
000000	011111111110	00111111110000
	011111111100	00111111111110
		01111111111110
		01111111111110
a1	a2	a3

Figure 3. Arbitrary structuring elements a1, a2 and a3

Grayscale opening by reconstruction is defined as follows using equation (1). Let I and J be two grayscale images defined on the same domain D_I such that $I \leq J$. The grayscale reconstruction by opening of I from J is obtained by iterative grayscale geodesic erosions of J above I until stability is reached.

$$\rho_I^*(J) = \bigwedge_{n \geq 1} \varepsilon_I^{(n)}(J) \quad (1)$$

where ρ^* represents the grayscale reconstruction by opening, \bigwedge represents iteration operator, ε represents the geodesic erosion, and n represents the number of iterations.

Grayscale closing by reconstruction is defined as follows using equation (2). Let I and J be two grayscale images defined on the same domain D_I such that $I \leq J$. The grayscale reconstruction by closing of I from J is obtained by iterative grayscale geodesic dilations of J under I until stability is reached.

$$\rho_I(I) = \bigvee_{n \geq 1} \delta_I^{(n)}(I) \quad (2)$$

where ρ represents grayscale closing by reconstruction, \bigvee represents the iteration operator, δ represents the geodesic dilation, and n represents the number of iterations.

The processed top hat is added to the original image and the processed bottom hat is subtracted from it. This image cleaning procedure is repeated three times with three different predefined arbitrary structuring elements. Now the input image I which is free from speckle noise and has not lost its features is obtained. Figure 4(a) shows an image with speckle noise and the cleaned image after applying the MMIC algorithm is shown in Figure 4(b), which is segmented using the proposed segmentation algorithm.



Figure 4. (a) Image before preprocessing; (b) Image after preprocessing

MMIC algorithm

Step 1. Repeat Step 2 to Step 9 three times.

Step 2. Let $X = \text{OCCO}(I, a_i)$ where I is the original image with noise and a_i is the arbitrary structure element. OCCO means a sequence of morphological operations namely opening, closing, closing and opening. X is the resulting image after applying OCCO.

Step 3. $T(x,y) = \begin{cases} I(x,y) - S(x,y) & \text{if } I(x,y) - S(x,y) > 0 \\ 0 & \text{if } I(x,y) - S(x,y) \leq 0 \end{cases} ; ;$

(x and y represents the row and column of pixels in the image.)

Step 4. Find $t(x,y)$ by thresholding $T(x,y)$ using the standard deviation of $T(x,y)$.

Step 5. Let $tcap =$ reconstruction by closing of t .

Step 6. $B(x,y) = \begin{cases} S(x,y) - I(x,y) & \text{if } S(x,y) - I(x,y) > 0 \\ 0 & \text{if } S(x,y) - I(x,y) \leq 0 \end{cases}$

Step 7. Find $b(x,y)$ by thresholding $B(x,y)$ using the standard deviation of $B(x,y)$.

Step 8. Let $bcap =$ reconstruction by opening of b .

Step 9. Modify I as $X + tcap - bcap$.

(The symbols $T, I, S, t, B, b, bcap$ and $tcap$ represent images.)

Segmentation

Segmentation is the next step applied on the preprocessed image. The segmentation component is expressed in terms of production rules, which capture the perceptual knowledge relevant to the domain. These rules will detect appropriate boundaries and pertinent regions in the image.

Outline of proposed segmentation algorithm

1. Read the original image.
2. Crop the unwanted areas from the input image.
3. Clean the image by using MMIC algorithm.
4. Find the end of the urinary bladder to locate the starting of the uterus within which the fibroid lies by fixing a threshold.
5. Make a binary image by selecting dark cluster of pixels in the range 0.005 to 0.3 which constitutes the fibroid region by applying knowledge-based rules.
6. If the number of regions is more than one, select one region by applying rules.
7. Define a diamond-shaped region in the image by dilating the region obtained in step 6.
8. Mark the pixels within the diamond-shaped area whose intensity falls in a specified range that is fixed according to the texture of the image.
9. Consider the biggest region in it and crop it to remove the extensions around it, if any.
10. Draw the contour around it.

Proposed segmentation algorithm

Step 1. Crop the original image to remove unwanted areas. The margin area is removed; only the image area is left. Clean the speckle noise in the cropped image by implementing MMIC algorithm.

Step 2. Find the starting row, starting column, ending row and ending column of the bladder by fixing a threshold obtained from the knowledge base.

Step 3. Find the uterus area within which the fibroid lies as follows.

a) Number of rows in the image > 260

i) If the ending row of the bladder is in the upper one quarter of the image or the starting column of the bladder $< \text{no. of columns}/2$, the bladder is either at the top or starts at the upper left. The uterus area is in the upper half of the image. The area starts at $(\text{no. of rows}/2-60, 70)$ and ends at $(\text{no. of rows}-30, 200)$.

ii) Otherwise, if the bladder end is in the middle of the image, the uterus area is in the middle of the image. The area starts at $(\text{no. of rows}/2-60, 70)$ and ends at $(\text{no. of rows}-30, 140)$.

b) Otherwise, if $\text{no. of rows} < 260$, the image is small and the area within which the fibroid lies is in the lower half of the image. The area starts at $(\text{no. of rows}/2, 70)$ and ends at $(\text{no. of rows}-30, 200)$.

Step 4. Search for the fibroid within the uterus area defined in Step 3 as follows.

Step 5. Find the count of pixels whose intensity is in the range 0.005-0.05. If the count is greater than 15, it could be the fibroid region; go to Step 8. Otherwise, it could not be the fibroid region and it is negligible; go to Step 6.

Step 6. Find the count of pixels whose intensity is in the range 0.005-0.155. If the count is greater than 15, it could be the fibroid region; go to Step 8. Otherwise, it could not be the fibroid region and it is negligible; go to Step 7.

Step 7. Find the count of pixels whose intensity is in the range 0.005-0.255. If the count is greater than 15, it could be the fibroid region; go to Step 8. Otherwise, it could not be the fibroid region and it is negligible; there is no fibroid and stop.

Step 8. The regions found by the steps above are displayed and the fibroid region is one among them.

Step 9. Remove the regions whose area is below 10 using morphological operation. This is because the diameter of an anechoic fibroid is not less than a centimetre.

Step 10. For each of the region do the following.

- a) Find centx_dist =difference between the x-coordinate of the centre of the image and the x-coordinate of the centroid of the region.
- b) Find centy_dist =difference between the y-coordinate of the centre of the image and the y-coordinate of the centroid of the region.
- c) Find max x1 =maximum x-coordinate of the region.
- d) Find min x1 = minimum x-coordinate of the region.
- e) If the number of rows in the image is less than 260, then the fibroid is in the lower half of the image.
 - i) If there are regions which are not near the top of the image (not within 80 rows) and whose $\text{centy_dist} \leq 75$, take it as the fibroid region.
 - ii) Otherwise, if there is any region which is not near the top with $\text{centy_dist} < 50$ and y-coordinate of the centroid < 200 with $\text{min x1} < 100$ and $\text{max x1} > 50$, take it as the fibroid region.
- f) Otherwise (if the image is not reduced much), if there are regions whose $\text{centy_dist} \leq 150$, find the biggest among them.

Step 11. Now only a part of the fibroid is found. Therefore, to find the entire fibroid region, do the following.

- a) Find the area of the fibroid region. If it is smaller than 500, a diamond-shaped structuring element enclosing the fibroid is created. The dilated region is adjusted as follows.
- b) If the y-coordinate of the centre of the dilated region is in the upper half of the image, adjust the maximum of x-coordinate such that it is not greater than 160. This is because the bladder will be at the right-hand side of the upper half.
- c) Otherwise, starting column is made as $\text{no. of columns}/2-20$. This is because when the fibroid is in the lower half of the image, the fibroid will not start at the leftmost position.

Step 12. The pixels of the original cleaned image corresponding to the pixels in the dilated region are to be considered for processing. Now the intensity of the pixels that constitute the fibroid region is determined as follows.

- a) The minimum intensity among the pixels is stored in min2 .
- b) The average of pixels in the fibroid region is found.
- c) If $\text{average} > 0.3$, set max_limit as $\text{average}-0.1$.
- d) Otherwise, if average is in the range 0.1-0.15, set max_limit as $\text{avg}+0.03$.
- e) Otherwise, if average is in the range 0.05-0.09 :
 - i) If the count of pixels is greater than 10000, set max_limit as $\text{avg}-0.01$.

ii) Otherwise, set max_limit as avg+0.05.

f) Otherwise, set max_limit as 0.05 + the first digit after the decimal point in the average.

Step 13. Pixels of the region whose intensity are in the range min2 to max_limit are marked.

Step 14. Contour of fibroid is drawn around the marked pixels.

Feature Extraction

The goal of feature extraction is to obtain representative features that can be used to determine the mode of treatment. For instance, if the size of the fibroid is very small, it can be treated by giving medicine, whereas if the size is big, it should be removed by surgery. The shape-based features, i.e. diameter, area and compactness, are the essential measures.

Diameter

It is measured and specified by the radiologist as horizontal and vertical diameters in centimetres. After segmenting the fibroid, the horizontal and vertical diameters are calculated in pixels and converted to centimetres.

Area

The area of the fibroid is the number of pixels inside the fibroid. It is used to specify the size of the fibroid. It can also be found by the formula $\pi \cdot a \cdot b / 2$, where a and b are the horizontal and vertical diameters.

Compactness

The compactness of a region is defined as the ratio of the square of the perimeter of a region to its area, i.e. $\text{compactness} = \text{perimeter}^2 / \text{area}$, where the perimeter is the distance around the boundary of the fibroid and the area is the number of pixels inside the fibroid.

Evaluation Criteria

There are two types of methods for image segmentation evaluation [25]. Analytical methods analyse and evaluate segmentation algorithms themselves by their principles and properties. Empirical evaluation methods measure the quality of segmentation results. Because empirical evaluation methods provide easy-to-interpret objective evaluations, only empirical methods are commonly used. Ideally, a segmentation result obtained from the algorithm would be compared with an expected segmentation known as the ground truth. The manual segmentations or ground truths are acquired from experts, often called gold standard.

The contour obtained from the segmentation algorithm is usually different from the one given by the expert. Every pixel in the output of the segmentation algorithm therefore belongs to one of the following classes: true positive (TP), true negative (TN), false positive (FP) or false negative (FN). These are the evaluation criteria to evaluate the performance of each algorithm. These terms are defined as follows.

TP: A recognised region that is correctly determined to be an object

FP: A recognised region that is incorrectly determined to be an object

TN: An unrecognised region that is correctly determined not to be an object

FN: An unrecognised region that is incorrectly determined not to be an object

The following evaluation measures have also been used to evaluate the performance of the proposed algorithm:

- 1) Pixel accuracy. It is defined as $(TP+TN) / (TP+TN+FP+FN) * 100 \%$. It measures the ratio of pixels/regions which are correctly identified to the total number of pixels/regions.
- 2) Specificity. It is defined as $TN / (TN + FP) * 100 \%$. This is the true negative rate. It measures the accuracy of a segmenting method in identifying all unmarked pixels/regions.
- 3) Sensitivity. It is defined as $TP / (TP+FN) * 100 \%$ and is also known as Recall. This is the true positive rate. It measures the accuracy of a segmenting method in identifying all marked pixels/regions.

RESULTS

The proposed algorithm was applied on 100 images of uterus with fluid-filled fibroids. The algorithm worked well on all images and gave good results. To evaluate the proposed segmentation algorithm, the same set of images were given to two radiologists who were asked to mark the fibroids. Figure 5(a) shows a sample output image produced by the implementation of the proposed algorithm. Figures 5(b,c) show the ground truths of the same sample image which were produced by expert 1 and expert 2 respectively. Tables 1-2 display results of performance evaluation of the proposed algorithm. The performance of the algorithm was measured using three evaluation criteria, viz. accuracy, sensitivity and specificity, by comparing the output of the proposed segmentation algorithm with the ground truths from expert 1 and expert 2 for 10 images. The performance of the algorithm was found to be very good as the average accuracy, sensitivity and specificity were above 95%.

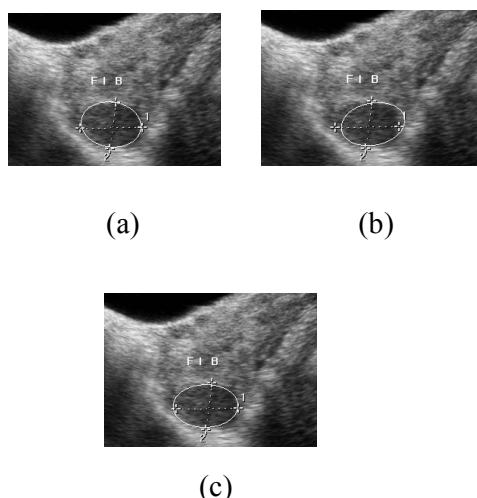


Figure 5. (a) Fibroid segmented by the algorithm; (b) Ground truth from expert 1; (c) Ground truth from expert 2

Table 1. Evaluation measures with respect to the ground truth from expert 1

Image	Accuracy (%)	Sensitivity (%)	Specificity (%)
Image1	98.02	94.16	98.16
Image2	95.55	95.40	95.56
Image3	95.76	100.00	95.64
Image4	97.89	87.55	98.09
Image5	91.75	91.98	91.73
Image6	98.89	92.42	99.12
Image7	95.87	97.14	95.81
Image8	96.86	99.07	96.74
Image9	97.73	91.85	97.97
Image10	97.06	98.05	97.01
Average	96.54	94.76	96.58

Table 2. Evaluation measures with respect to the ground truth from expert 2

Image	Accuracy (%)	Sensitivity (%)	Specificity (%)
Image1	97.83	96.86	97.86
Image2	95.55	95.40	95.56
Image3	96.27	99.65	96.15
Image4	97.86	99.49	97.83
Image5	96.42	92.19	97.05
Image6	99.00	93.08	99.22
Image7	97.42	92.53	97.76
Image8	96.86	99.07	96.74
Image9	97.73	91.85	97.97
Image10	96.92	96.88	96.93
Average	97.19	95.70	97.31

CONCLUSIONS

The subjective appearance of the output image was good. The performance of this algorithm was also very good. It was fully automatic and did not require human intervention. It was fast compared to such segmentation procedures as set methods. There was no need to give the seed point to start segmentation.

REFERENCES

1. L. Vincent, "Morphological grayscale reconstruction in image analysis applications and efficient algorithms", *IEEE Trans. Image Process.*, **1993**, 2, 176-201.

2. M. Karamam, M. Kutay and G. Bozdagi, "An adaptive speckle suppression filter for medical ultrasonic images", *IEEE Trans. Med. Imaging*, **1995**, 14, 283-292.
3. R. A. Peters II, "A new algorithm for image noise reduction using mathematical morphology", *IEEE Trans. Image Process.*, **1995**, 4, 554-568.
4. M. A. Schulze and Q. X. Wu, "Noise reduction in synthetic aperture radar imagery using a morphology-based nonlinear filter", Proceedings of Digital Image Computing: Techniques and Applications, **1995**, Brisbane, Australia, pp. 661-666.
5. P. Salembier and J. Serra, "Flat zones filtering, connected operators and filters by reconstruction", *IEEE Trans. Image Process.*, **1995**, 4, 1153-1160.
6. D. L. Pham, C. Xu and J. L. Prince, "A survey of current methods in medical image segmentation", *Annu. Rev. Biomed. Eng.*, **2000**, 2, 315-337.
7. J. A. Noble and D. Boukerroui, "Ultrasound image segmentation: A survey", *IEEE Trans. Med. Imaging*, **2006**, 25, 987-1010.
8. A. F. C. Infantosi, L. M. S. Luz, W. C. A. Periera and A. V. Alvarenga, "Breast ultrasound segmentation using morphological operators and a Gaussian function constraint", *IFMBE Proc.*, **2008**, 20, 520-523.
9. J. Shan, J. D. Cheng and Y. Wang, "A novel automatic seed point selection algorithm for breast ultrasound images", Proceedings of International Conference on Pattern Recognition, **2008**, Tampa, Finland, pp. 1-4.
10. A. Thakur and R. S. Anand, "A local statistics based region growing segmentation method for ultrasound medical images", *Int. J. Signal Process.*, **2005**, 1, 141-146.
11. M. Aleman-flores, P. Aleman-flores, L. Alvarez-leon, R. Fuentes-pavon and J. Santanamontesdeoca, "Filtering, segmentation and feature extraction in ultrasound evaluation of breast lesions", Proceedings of Image Processing for Medicine, **2008**, Berlin, Germany, pp.168-172.
12. W. Gomez, L. Leija, W. C. A. Pereria and A. F. C Infantosi, "Anisotropic diffusion filtering and average radial derivative to segment ultrasound like images", Proceedings of the XXI Brazilian Congress of Biomedical Engineering, **2008**, Salvador, Brazil, pp.1410-1413.
13. F. Meyer and S. Beucher, "Morphological segmentation", *J. Visual Commun. Image Represent.*, **1990**, 11, 21-46.
14. R. C. Gonzalez and R. E. Woods, "Digital Image Processing", 2nd Edn., Prentice Hall, Upper Saddle River, NJ, **2002**, pp. 617-624.
15. A. Bleau and L. J. Leon, "Watershed-based segmentation and region merging", *Comput. Vision Image Underst.*, **2000**, 77, 317-370.
16. I. Levner and H. Zhang, "Classification-driven watershed segmentation", *IEEE Trans. Image Process.*, **2007**, 16, 1437-1445.
17. L. Vincent, "Morphological area openings and closings for grayscale image", Proceedings of NATO Shape in Picture Workshop, **1992**, Driebergen, The Netherlands, pp. 197-208.
18. L. Vincent, "Grayscale area openings and closings, their efficient implementation and applications", Proceedings of EURASIP Workshop on Mathematical Morphology and its Applications to Signal Processing, **1993**, Barcelona, Spain, pp. 22-27.

19. H. T. Nguyen, M. Worring and R. van den Boomgaard, "Water snakes: Energy-driven watershed segmentation", *IEEE Trans. Pattern Anal.*, **2003**, 25, 330-342.
20. M. Wirth, D. Nikitenko and J. Lyon, "Segmentation of the breast region in mammograms using a rule-based fuzzy reasoning algorithm", *ICGST-GVIP J.*, **2005**, 5, 45-54.
21. E. A. Ince and S. A. Ali, "An adept segmentation algorithm and its application to the extraction of local regions containing fiducial points", *Lect. Notes Comput. Sci.*, **2006**, 4263, 553-562.
22. E. A. Ince and S. A. Ali, "Rule based segmentation and subject identification using fiducial features and subspace projection methods", *J. Comput.*, **2007**, 2, 68-75.
23. J. Yao, C. David, W. Lu and P. Ahalya, "Uterine fibroid segmentation and volume measurement on MRI", *Proceedings of SPIE on Medical Imaging 2006: Physiology, Function and Structure from Medical Images*, **2006**, 6413, 640-649.
24. J.-P. Guyon, M. Foskey, J. Kim, Z. Firat, B. Davis and S. Aylward, "Volume estimation and tracking over time: Framework and validation", *Lect. Notes Comput. Sci.*, **2003**, 2879, 142-149.
25. Y. J. Zhang, "A survey on evaluation methods for image segmentation", *Pattern Recognit.*, **1996**, 29, 1335-1346.